

Elastic compressive-flexural-torsional buckling in structural members

W.J. Raven, J. Blaauwendraad and J.N.J.A. Vamberský

Faculty of Civil Engineering and Geosciences, Delft University of Technology, the Netherlands ¹

This article presents insight into the stability check for members loaded in a combination of compression and bending, in which - due to 2nd-order effects - also torsion occurs. A key decision in the opinion of the authors is the introduction of the stability parameter n^* as the ratio of the total displacement and the 2nd-order part of displacement. They believe that this quantity can fulfill an 'alarming function' when judging the stability of structural members. An iteration procedure in a number of clearly distinct steps results into a general formula for n^* , in which all necessary data concerning member properties and load cases are covered. The member safety is inspected by a unity check, which relates occurring stresses to strength requirements. Also checks on displacement limits are described.

This new method for compressive-flexural-torsional buckling is applicable for all existing building materials in structural engineering as long as elasticity is involved.

Essentially, the calculations can be done in a short time using a pocket calculator, without the use of other utilities. It has been deliberately chosen not to elaborate the derived formulas too far, in order to preserve a clear view on cohesion and procedure.

Key words: Building structures, structural members, stability, strength, stiffness, column buckling, flexural-torsional buckling, bending, twist

1 Introduction

The assessment of the stability, stiffness and strength of members loaded in bending and compression mostly yields complicated analyses, in which an effective combination of simplicity and accuracy often is not possible. In the course of years several advanced

¹ This article is based on the doctoral thesis of the first author, which he completed in 2006 at Delft University of Technology under supervision of the two other authors [14].

methods have been developed, which facilitate the simulation of the flexural-torsional buckling and/or column buckling of (members of) structures.

Early studies were done in the USA by Timoshenko [1], Timoshenko and Geere [2], Bleich [3], later on followed by a fundamental work of Chen and Atsuta [4] and an even more recent American/Italian work of Bazant and Cedolin [5]. Part of the book of Chen and Atsuta was contributed by the Australian author Trahair, who himself also wrote a book on flexural-torsional buckling [6]. Series of German studies can be reported, written by Brüninghoff [7], Blass [8], Pauli [9], and Lohse [10] as well as a Norwegian contribution from Eggen [11], the contribution from Van der Put to the Dutch timber code [12] and a Dutch contribution from Van Erp [13]. Some of studies referred to are based on a more or less complete set of differential equations; others start from virtual work considerations and series development of displacement fields. Some result in closed-form solutions, others apply numerical methods.

In case differential equations are used, they are in great majority linear ones. One of the rare exceptions is reported by Trahair [6] and also in Chen et al. [4], where nonlinear equations appear to yield improved results, which are in most cases more efficient than achieved by the linear equations. The nonlinear equations take account of the effect of the displacement in the direction of the major cross-section axis. The linear approach is conservative for members with a major stiffness direction, which is dominant over the stiffness in the minor direction and the twisting stiffness. As a consequence, timber beam sections and *I*-shaped or *H*-shaped steel sections can safely be studied by the linear approach. So, this will be done in the present study. The advanced nonlinear approach only needs to be applied in case of more or less square box sections, which are out of scope here. For such sections displacement in the major stiffness direction is not small if compared to the lateral displacement, hence, therefore its effect can not be neglected anymore.

In view of so many studies based on the classic linear starting points, why, yet, a new approach to this issue? The answer to this question results from the experience that application of tools, supplied by others, like computer programs, complicated formula, tables and graphs, indeed can rapidly yield results, but seldom provide good insight in the real behavior of spanning structures. One reason is that some studies just produce a formula for the critical load of perfectly straight members, which does not offer a helping hand in the assessment of members in practical situations for a given load. Another reason is the way in which formulas are elaborated. In many publications and design codes the

working-out in detail unpleasantly hides from view the background of the formulas, hence insight is obstructed. Moreover, the working-out is different for different materials, very confusing for structural engineers who design structures in all existing building materials. Apart of that, the common calculation methods are mainly fit for checking purposes, without offering assistance how to optimize the structural design. There is a need for an analysis type, as simple and conveniently-arranged as possible, which also can serve as a design instrument.

It is expected that a simple, reliable analysis method, not requiring special tools, contributes to insight in structural behavior and time saving in design and analysis of structures and members thereof.

The present study started with an attempt to make stability formula's in the Dutch code for timber engineering accessible through tables and graphs. At a closer look, most other codes of practice appear, regardless of big differences, to be based on the same starting points. However, often they are elaborated in so much detail that the resulting formulas can only be applied by the use of computers, and, as a consequence, the logic of the formulas and the related factors and coefficients has completely disappeared. The designers can not see anymore the wood for the trees.

This justifies the fresh analysis to again clarify stability behavior of members and timely stop elaboration of the formula at stake in too much detail, before they become too complicated.

As a result the doctoral thesis "New vision on flexural-torsional buckling, stability and strength of structural members" has been written [14]. If here is written 'new', this does not particularly regard the reformulation of starting points or the derivation of the differential equations, though they were anew derived from scratch in the dissertation. Evenly, it is not claimed that all results are obtained for the first time, though a number indeed are original. Rather, it is believed that the alternative handling of the relations and the way in which solutions have been obtained is innovative, refreshing, revealing and alerting.

2 Starting points

2.1 Member types, loading and member end conditions

We start from a straight prismatic member of double-symmetric rectangular or *I*-shaped cross-section. The member axis coincides with the *x*-axis of an orthogonal set of axes *x, y, z*. The *y*-axis is in the 'weak' direction of the cross-section and the *z*-axis in the 'strong' direction.

These members are supported by fork supports at the ends and are loaded by a homogeneously distributed load q_z (whether or not applied eccentrically), alternatively combined with an axial compressive force F_c in the x -direction, see Figure 1.

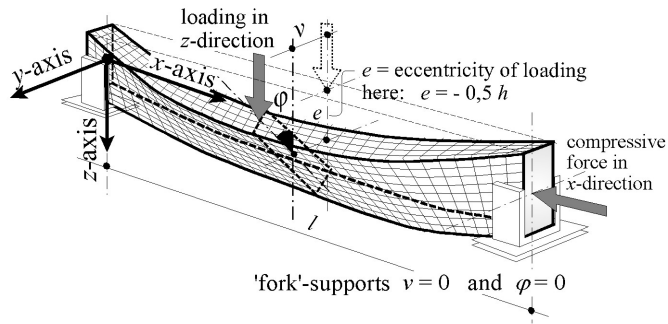


Figure 1: Structural member on two supports

In [14] also clamped members, members continuing over supports and cantilever beams are discussed, as well as other types of loading.

Flexural-torsional buckling may occur at a combination of a small stiffness in the lateral-to-load direction and small torsion stiffness. However, to the opinion of the authors, such structures can only responsibly be applied if no external torque load or load in the weak direction occurs. Therefore, they choose not to include such load types and purposely have restricted to load application in the major stiffness direction only.

The response of the members is studied in a spread sheet program, in which the interaction of deflections, loads and 2nd-order effects is investigated in nine steps and finally is computed in an iterative way. The iteration method offers interesting possibilities to analyze several member types and load combinations in a rather simple and conveniently-arranged way. To the knowledge of the authors no such method was applied before to examine the flexural-torsional buckling of members. Options of spread sheet programs to visualize results in graphs have extensively been used, timely revealing unrealistic results due to errors in programming if present. This visual check, in combination with each wanted number of iterations, is a guarantee for a big accuracy.

2.2 Sign conventions

For the used notations see Appendix.

The chosen sign conventions are shown in Figure 2.

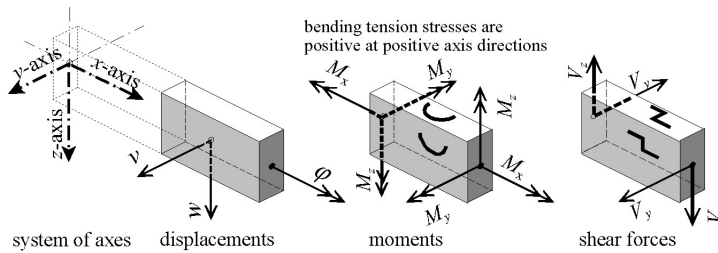


Figure 2: Sign conventions

- Moment M_y around the y -axis causes a tensile bending stress at the positive z -side of the cross-section; corresponding deflection w in the direction of the z -axis.
- Moment M_z around the z -axis causes a tensile bending stress at the positive y -side of the cross-section; corresponding deflection v in the direction of the y -axis.
- In a section face with the normal in the positive x -direction:
 - the vector of the twisting moment M_x is parallel to the positive x -axis,
 - the shear force V_z acts in the direction of the positive z -axis.

2.3 Assumptions

1. The classical beam theory is presupposed, including the statement of plane cross-sections after loading. A linear relationship exists between strains and displacements.
2. Only deflection due to bending and rotation due to torsion are accounted for. Shear displacement is neglected.
3. The influence of geometric imperfections and inhomogeneous effects are taken into account by assuming an initial sine-shaped deflection diagram. The amplitude (top-value) of this initial deflection is taken from the applying design code.
4. Initial rotation is not supposed here, because apparently twisted members can be rejected at construction or can be mounted to the fork supports in such a way that the starting rotation at mid-span is practically zero. For the rest, if wished, nonzero rotations can be easily included.
5. Two limit states are considered at which the effect of the applied loads and the response of the structure do not exceed the set of relevant requirements:
 - SLS (serviceability limit state), with requirements to the displacement of the structure at supposed usage.
 - ULS (ultimate limit state), with requirements to structural safety.

6. Interaction of load, stiffness and displacements causes 2nd-order stresses and displacements (deflections and rotations), which influence each other.
7. Because the studied structures are considered inapt for external (1st-order) torque load or load in the minor direction these loads are not applied. Nevertheless, nonzero torsion moments M_{t2} and bending moments M_{z2} will occur as 2nd-order moments due to load in the major direction.
8. The following general relations follow from elastic beam theory:

$$\text{strength: } \sigma_c = \frac{F_c}{A} \quad \sigma_{my} = \frac{M_y}{W_y} \quad \sigma_{mz} = \frac{M_z}{W_z} \quad \sigma_{mt} = \frac{M_t}{W_t} \quad (1)$$

$$\text{stiffness: } w'' = -\frac{M_y}{EI_y} \quad v'' = -\frac{M_z}{EI_z} \quad \varphi' = \frac{M_t}{GI_t} \quad (2)$$

herein each prime indicates a derivative with respect to x .

The bending stiffnesses EI_y and EI_z can be simply borrowed from classic elastic beam theory and need no further explanation. The torsion stiffness GI_t needs more attention, because the torsion moment exists of three components, and so does the torsion stiffness:

- a. One is the torsion stiffness according to De St. Venant; only shear stresses act in the member.
- b. The second is the influence of the normal force F_c on the torsion (Wagner effect).
- c. The third one is the warping resistance of the member, due to the flexural stiffness of the flanges, at which both shear stresses and bending stresses occur in the cross-section.

The total torsion moment can be written as:

$$M_t = M_{tor} + M_{tF} + M_{tw} \quad (3)$$

- ad a. Herein the 'pure' torsion component is:

$$M_{tor} = GI_{tor} \varphi' = W_{tor} \bar{\sigma}_{tor} \quad (4)$$

The torsion second-order moment I_{tor} and torsion section modulus W_{tor} are of particular interest for members. In case of circular and strip-like cross-sections they can be calculated in an easy way, otherwise tables or approximation formulas must be applied.

- ad b. The Wagner effect implicates a reduction of the square of the critical beam buckling moment with a factor $(1-F_c/F_t)$ where F_c is the normal force and F_t the torsion buckling force, see Trahair in [4] and [6]. The influence of the Wagner effect is of interest only in case of large normal forces. High compressive stresses reduce the torsion stiffness substantially. This will be the case for short wide members, because the compressive stress in slender members must be small in order to avoid column buckling. For the practical cases of timber beams and steel section of *I*- and *H*-shape considered in this study, the reduction is in the order of 1 percent or less. Therefore, we do not consider this effect in the present study.
- ad c. The third component of the torsion moment is due to the couple of two flange shear forces, see Figure 3.

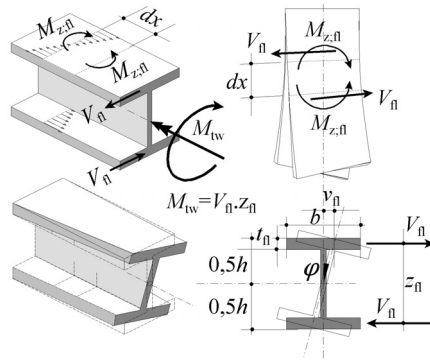


Figure 3: Displacements due to bending of the flange and warping of the profile

In each flange a bending moment M_{fl} occurs, which can be calculated from:

$$V_{fl} = \frac{dM_{z,fl}}{dx} = \frac{d(-EI_{fl}v_{fl}''')}{dx} = -EI_{fl}v_{fl}''''$$

In case of a non-deformable cross-section it holds: $\varphi = \frac{v_{fl}}{0,5z_{fl}}$ hence:

$$v_{fl}'''' = 0,5z_{fl}\varphi''''$$

Choosing the approximation: $I_{flz} \approx 0,5I_z$, and $z_{fl} \approx h$

we obtain the warping component of the twisting moment:

$$M_{tw} = V_{fl}z_{fl} \approx -EI_{fl} \times 0,5h\varphi'''' h = -0,25EI_z h^2 \varphi'''' = -EI_w \varphi'''' \quad (5)$$

where: $I_w = 0,25I_2h^2$

Hence, summing up equation (4) and (5), the twisting moment can be written as:

$$M_t = GI_{tor}\varphi' - EI_w\varphi''' = GI_{tor}\varphi' \left(1 - \frac{EI_w\varphi'''}{GI_{tor}\varphi'} \right) \quad (6)$$

Correct determination of the warping component implies substitution of the term φ''' / φ' in the differential equation and solving it. In [14] this is worked-out for a large number of cases, at which it appeared that this term can practically be considered constant, which simplifies the analysis remarkably. To give an example, for the case of the frequently occurring sine-shaped distribution of the rotation, it holds for a member span l :

$$\frac{\varphi'''}{\varphi'} = -\frac{\pi^2}{l^2}$$

After introduction of:

$$C_{tw} = \frac{\pi^2 EI_w}{l^2 GI_{tor}} \quad (7)$$

the effective total torsion stiffness GI_t can be simply written as:

$$GI_t = GI_{tor} (1 + C_{tw}) \quad (8)$$

This formula is sufficiently accurate for most occurring load cases and members on two supports in design practice and is in concordance with the approach in some codes of practice.

The authors are attached to underline their awareness that many of the starting assumptions in this section have been previously made by other researchers. A number of them are the basis of many a code of practice. Furthermore, not all assumptions are serious restrictions. To mention a few, initial imperfections for the rotation could easily be inserted in the procedure if wanted. The same holds true for load in the minor stiffness direction and a torque load. Otherwise, putting a requirement to the displacement in the minor direction in the serviceability limit state will not occur in many codes of practice, for example the Eurocode for timber structures. So, if not relevant, one may quickly step-over such an item in the present article.

3 Basis equations and method of analysis

3.1 Displacements

The total displacement field exists of displacements w in the z -direction, displacements v in the y -direction and rotations φ around the x -axis. For reasons of simplicity we first have a closer look at the displacement v . The total displacement v exists of three components, shown in Figure 4:

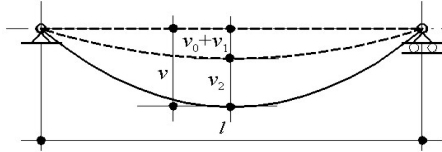


Figure 4: 1st - and 2nd order displacements

$$v = v_0 + v_1 + v_2 \quad (9)$$

where:

v_0 = initial deflection,

v_1 = 1st-order displacement due to the external load,

v_2 = 2nd-order displacement due to interaction of loads and final displacement.

In classic studies it is common practice to define, as a starting point, the ratio $n = F_E / F_c$ where F_E is the critical Euler buckling load and F_c the occurring compressive load.

From this definition one easily derives, as a consequence, the relations:

$$v = \frac{n}{n-1}(v_0 + v_1), \quad v_2 = \frac{1}{n-1}(v_0 + v_1), \quad v_2 = \frac{1}{n}v. \quad (10)$$

The last relationship in (10) refers the total displacement to the second-order displacement v_2 , in which the latter is an important quantity in determining the bending moment in the minor direction.

It appears appropriate to exchange the starting point and the consequence. In the present article we introduce the newly defined stability parameter:

$$n^* = \frac{\bar{v}}{\bar{v}_2} = \frac{\text{'top value' of the total displacement}}{\text{'top value' of the 2nd-order part of the total displacement}} \quad (11)$$

The asterisk superscript is purposely added to n in order to distinguish it from the commonly used definition of n as the ratio of the critical load and the occurring load in column buckling theory. It is true, this definition is not common, but this adaptation of the definition turns out to be the key to a very efficient and orderly calculation of the 2nd-order effects. In (9) no bars have been used on top of the displacement symbols, which suggests that the relationships are true for each position along the member. This is true if we start from sine-shaped initial displacements v_0 and first-order displacements v_1 . In case of general loading types this will not be the case, reason why the amplitudes are used. In fact, we can further refine (10), because it is appropriate to distinguish between:

$$n_y^* = \frac{\bar{w}}{w_2} \quad \text{and} \quad n_z^* = \frac{\bar{v}}{v_2} \quad (12a), (12b)$$

The reader is reminded here of the definitions for displacements and moments.

The displacement v is in the direction of the y -axis due to a moment M_z around the z -axis. Similarly, the displacement w in the z -direction is due to a moment M_y around the y -axis, see Figure 2.

In case exclusively 2-D Euler column buckling occurs, n^* and n are equal to each other. It is shown in [14] that the influences of the displacement w and n_y^* are practically negligible for 3-D buckling cases, a confirmation of Trahair's work in [4] and [6]. However, the 2nd-order displacements v_2 and the connected moments M_{z2} are of big importance.

So, attention is exclusively paid to the determination of the stability parameter n_z^* and its consequences. The general relation between the displacements v_0, v_1, v_2 and v is now easily derived from the end state, according to the scheme in Table 1:

Table 1: Relations between 1st- and 2nd-order displacements

- start (1st-order):	$\bar{v}_0 + \bar{v}_1$	
- additional (2nd-order):	$\bar{v}_2 = \frac{\bar{v}}{n^*}$	(13)
- total:	$\bar{v} = \bar{v}_0 + \bar{v}_1 + \frac{\bar{v}}{n^*}$	
- end state:	$\bar{v} = (\bar{v}_0 + \bar{v}_1) \frac{n^*}{n^* - 1}$	(14)

The derived *amplification factor* $n^*/(n^* - 1)$ in the scheme is the factor, familiar to structural engineers, to calculate the increase of the initial value to the end value as a consequence of the second-order effect, as earlier occurred in the first relationship of (10).

It is common practice to use a sine shape for the v_0 -diagram. The shape of the v_1 -diagram is fully dependent on the applied load and follows from the elastic beam theory. The shape of the v_2 -diagram results from the second-order moments, which, in their turn, are due to the interaction of the occurring forces and the v -diagram, itself in its turn the resultant of all mentioned displacements.

From what precedes it may be clear that the displacement diagrams (v_0 , v_1 , v_2 and v) have seldom the same shape. As a consequence, the problem mostly becomes too complicated for a closed-form mathematical solution. However, because of the here introduced definition of n^* , it is sufficient to know the ratio of the top values of the v_2 - and v -diagram for an accurate calculation of the occurring 2nd-order effects.

3.2 *Interaction of forces, moments and displacements*

Here we study the relation between bending moments, axial compressive force and deflections and also the relation between torsion moments and rotations, and their interaction by 2nd-order effects. As was argued before (section 2.4 sub 7) no external twisting load and lateral load in the weak direction are taken into account.

The total moments to account for in a loaded member are composed of:

- M_{y1} : 1st-order moments, directly due to the loads,
- M_{y2} , M_{z2} , M_{t2} : 2nd-order moments, due to the total displacements w , v and φ .

The total displacement field (deflections and rotations) of the considered member is composed of:

- w_0 , v_0 : initial displacements (supposing a stress-less member, hence: $M_0 = 0$),
- w_1 : displacements due to 1st-order moments,
- w_2 , v_2 , φ_2 : ditto, due to 2nd-order moments.

Therefore, a complicated interaction pattern comes into being:

- displacements
- moments
- hence 2nd-order displacements
- hence 2nd-order moments
- etcetera,

as shown in the scheme of Figure 5.

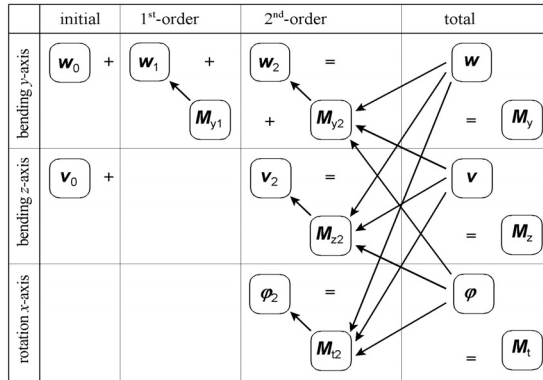


Figure 5: Interactions of displacements and moments

All displacements cause a (very small) rotation of the considered cross-section:

A rotation around the x-axis causes the cross-section to

rotate in its plane over an angle φ . It holds:

$$\sin \varphi = \tan \varphi = \varphi \quad \cos \varphi = 1$$

A deflection v in the direction of the y-axis (bending

around the z-axis) causes the cross-section to rotate over

an angle v' . It holds:

$$\sin v' = \tan v' = v' \quad \cos v' = 1$$

A deflection w in the direction of the z-axis (bending

around the y-axis) causes the cross-section to rotate over

an angle w' . It holds:

$$\sin w' = \tan w' = w' \quad \cos w' = 1$$

In case of a member on two fork supports forces, moments and deflections can occur as depicted in Figure 6:

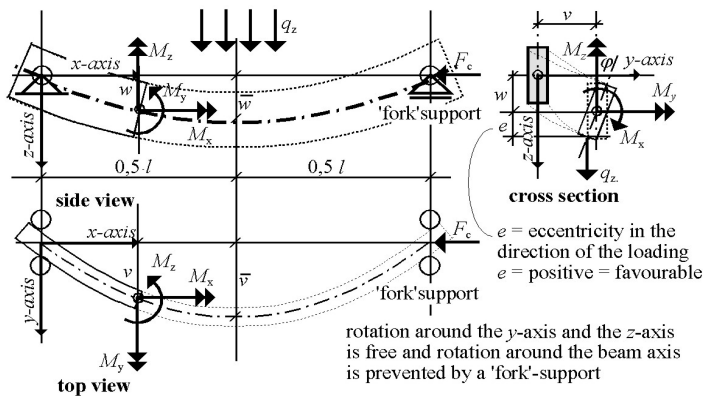


Figure 6: Simply supported member

Due to the 3-D deflections and rotations of all cross-sections, the moments can be resolved in the directions parallel and perpendicular to the member axis. The relations between moments, deflections and rotations are shown in Figure 7.

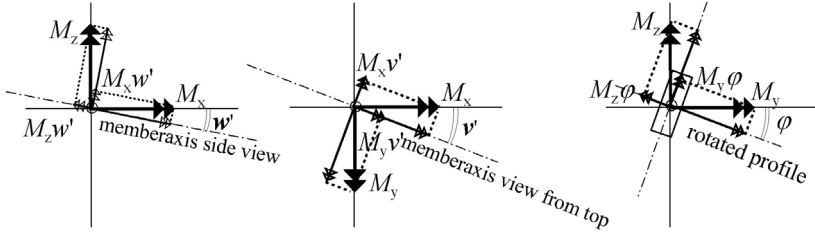


Figure 7: Components of moments in directions w' , v' and φ

From this figure it is read:

- deflection w causes 2nd-order bending moment M_{z2} and twisting moment M_{t2}
- deflection v causes 2nd-order bending moment M_{y2} and twisting moment M_{t2}
- rotation φ causes 2nd-order bending moment M_{y2} and bending moment M_{z2}

Hence, the resolved moment vectors and the eccentrically acting axial force (due to the displacements) cause the next 2nd-order moments:

$$\begin{cases} M_{y2} = +F_c w \\ M_{z2} = +F_c v + M_{y1} \varphi \\ M_{t2} = +M_{y1} v' + M_{x2} \text{ *)} \end{cases} \quad (15)$$

- *) The component M_{x2} is due to the combination of the (possibly eccentric) load in z -direction and the displacement v and rotation φ , which will be elaborated later on.

These moments cause displacements (deflections and rotations) of the 2nd-order, which on their turn again influence the moments (jointly with the displacements of the 1st-order). No stresses are associated with the initial deflections, hence no 1st-order moments. The elementary relationships between on the one hand curvatures and twists and on the other hand bending and twisting moments are as follows:

$$\begin{cases} M_{y,tot} = M_{y1} + M_{y2} = -EI_y (w_1'' + w_2'') \\ M_{z,tot} = M_{z1} + M_{z2} = -EI_z (v_1'' + v_2'') \\ M_{t,tot} = M_{t1} + M_{t2} = GI_t (\varphi_1' + \varphi_2') \end{cases} \quad (16)$$

The relations between moments and displacement can be written as a set of coupled differential equations as shown in Table 2:

Table 2: Relations between moments and displacements

		external moments		internal moments	
		1 st -order	2 nd -order	1 st -order	2 nd -order
bending around	y -axis	$M_{y,tot} = M_{y1}$	$+F_c w$	$= -EI_y w_1''$	$-EI_y w_2''$
bending around	z -axis	$M_{z,tot} =$	$F_c v + M_{y1} \varphi$	$=$	$-EI_z v_2''$
rotation around	x -axis	$M_{t,tot} =$	$M_{y1} v' + M_{x2}$	$=$	$GI_t \varphi_2'$

(17)

Now an important decision can be taken. The internal and external 1st-order terms are completely equal and cancel-out. In solving the equations just the 2nd-order and total displacements are kept:

$$\begin{cases} M_{y2} = F_c w & = -EI_y w_2'' \\ M_{z2} = F_c v + M_{y1} \varphi & = -EI_z v_2'' \\ M_{t2} = M_{y1} v' + M_{x2} & = GI_t \varphi_2' \end{cases} \quad (18a)$$

These relationships may look simple, but it is practically impossible to find solutions without help of numerical methods. These relationships will be the basis of the subsequent elaboration in this article. The resting mutual relations between displacements and moments have been remarkably reduced as is easily seen from a comparison of the new scheme in Figure 8 with the preceding scheme in Figure 5.

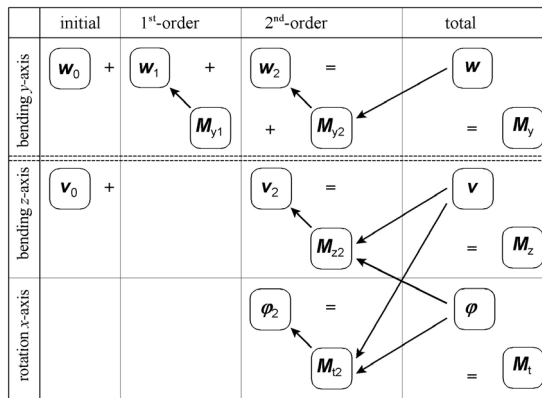


Figure 8: Reduced interaction scheme of displacements and moments

It is concluded that the displacement w in the strong direction and its connected 2nd-order effects have no influence on the flexural-torsional buckling and can (if wanted) be

calculated independently of v and φ . The displacement v in the weak direction and the rotation φ keep dependent on each other, but are not influenced by displacements w , which simplifies their calculation. Hence only the second and third equation of (18a) are relevant and they can be written as:

$$\begin{cases} EI_z v_2'' + F_c v + M_{y1} \varphi = 0 \\ M_{y1} v' + M_{x2} - GI_t \varphi_2' = 0 \end{cases} \quad (18b)$$

3.3 Analysis methods

In spite of the simplification a pure mathematical closed-form solution of the derived equations is only possible in a limited number of special load cases, such as the combination of an axial compressive force F_c and a homogeneous bending moment M_{y1} due to two equal opposite moments at the member ends.

Therefore, we look for a good approximation for the most occurring load cases in real practice. The application of numerical methods, with aid of spread sheet programs, is an effective instrument for the purpose. The interaction between the moments and displacements will be analyzed by the execution of an iteration process, consisting of:

- Assumption of the shape of the displacement diagram,
- Calculation of the consequences thereof (moments),
- Calculation of the 2nd-order displacements due to the moments,
- Check the match of the resulting and assumed displacements,
- Repetition, if necessary, up to satisfactory match.

In the consulted literature critical loads (eigenvalues of the system) usually are derived from differential equations. In fact, it is less interesting to choose the critical load as our goal; one better can focus onto a reliable prediction of the structural behavior at increasing load.

If one starts from an initial displacement, at first no stability problem does exist at all, but the material strength is always decisive for the load bearing capacity of the member. It then is important not to base the calculation on theoretical straight members, but to presuppose a certain measure of imperfection as occurring in practical circumstances. Many codes of practice provide relevant information for this initial deflection.

For a simple and unambiguous prediction of the flexural-torsional buckling behavior of straight members three phases must be considered:

1. By way of an iteration method the value of the stability parameter n_z^* is calculated.
2. The influence of this quantity n_z^* to the amount of the 2nd-order effects is investigated.
3. Finally, the decisive stress to be expected is calculated and checked upon the applying code of practice.

4 Iteration method – scheme steps

The investigated cases have been elaborated with the spread sheet program Quattro-Pro 9, which was also used for the graphs of results. For the detailed set-up of the produced spread sheets it is referred to [14].

Here the main lines of the process are discussed.

- The procedure starts with an estimate of the deflection v and its derivative v' .
- Then the twisting moment M_{t2} , the twist ϕ and the rotation φ are computed from the rotation equation.
- The 2nd-order moment M_{z2} and curvature v_2'' are computed from the bending equation.
- Two times integration yields the displacement v_2 .
- Finally, the quantity n_z^* is obtained as the ratio of \bar{v} and \bar{v}_2 .

The match in shape of starting and final displacements can be checked automatically by performing the computations iteratively. Each next iteration starts from the results of the preceding one, hence the results become increasingly more accurate. The process can stop if the results of successive iterations are sufficiently close. See Table 3 and Figure 9.

In the case of a constant moment all displacement components are sine-shaped (or cosine-shaped) and in fact no iteration is needed because v and φ can be solved directly from the governing differential equations.

On basis of the obtained value of n_z^* the 2nd-order effect can be derived, after which the total stress can be determined and checked against the applying strength data.

Table 3: Scheme iteration steps

1.	estimate deflection diagram:	$v =$ total displacement (almost sine shaped) at start: $\varphi = 0$
2.	from this:	twisting moment M_{t2}
3.	from this:	rotation φ around x -axis: $\varphi = \int_0^x \frac{M_{t2}}{GI_t} d\xi$
4.	from 1 and 3:	2 nd -order moment M_{z2} : $M_{z2} = M_{y1}\varphi + F_c v$
5.	from this:	curvature around z -axis: $v_2'' = -\frac{M_{z2}}{EI_z}$
6.	from this:	displacement 2 nd -order: $v_2 = \int_0^x \int_{0.5/l}^{\zeta} v_2'' d\xi d\zeta$ now the primes indicate derivatives with respect to ξ and ζ
7.	new:	total displacement: $v = (v_0 + v_1) + v_2$
8.	comparison and repetition:	the process of steps 2 up to 8 is executed iteratively until shape and size of v and v_2 do not change anymore.
9.	finally:	stability parameter: $n_z^* = \frac{\bar{v}}{\bar{v}_2}$

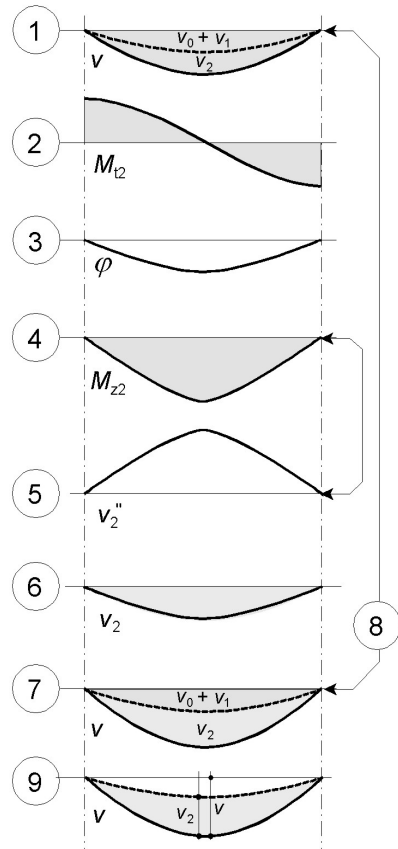


Figure 9: Iteration process in 9 steps

In this article we elaborate the case of a member on two fork supports, loaded by a homogeneously distributed load q_z in combination with an axial load F_c .

The load q_z is applied eccentrically at a distance e from the member axis and keeps vertical during rotation and transverse displacement of the cross-section, and moves in y -direction. The forces F_c at both ends do not change of direction either nor displace in y -direction, see Figure 10:

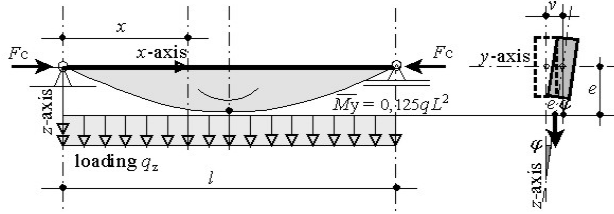


Figure 10: Simply supported beam under uniform loading

The calculation of the twisting moment in the second step of the scheme in Table 3 and Figure 9 follows from the last equations of (15) and (18a) and (18b):

$$M_{t2} = \int_{0,5l}^x M'_{t2} d\xi = \int_{0,5l}^x (M_{y1}v' + M_{x2})' d\xi$$

The derivative of this twisting moment is: $M'_{t2} = (M_{y1}v')' + M'_{x2} = M_{y1}v'' + M'_{y1}v' + M'_{x2}$

In [14] it is derived that: $M'_{x2} = -V_z v' + q_z e \varphi$ wherein: $V_z = -M'_{y1}$.

So the derivative of the twisting moment can be calculated from:

$$M'_{t2} = M_{y1}v'' + q_z e \varphi \tag{19}$$

This 'increase' of the twisting moment is used in the second step of the scheme in order to calculate by (numerical) integration the distribution of the twisting moment over the length of the member.

The other steps in the scheme need no further explanation.

The systematic development is in the 9 following steps as shown in Table 4.

Table 4: Iteration process in nine steps

1. Deflection:

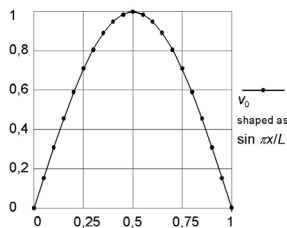


Figure 11a: v_0

It is started with $\varphi = 0$ and a sine shape deflection

$$\text{diagram: } v_0 = \bar{v}_0 \sin \frac{\pi x}{l} \tag{20}$$

In the next iterations a 2nd-order deflection v_2 is added, which will become increasingly more accurate, and the rotation φ will have become unequal zero. The calculation result is obtained (after sufficient iterations):

$$v = v_0 + v_2 = k_{1a} \bar{v} \sin \frac{\pi x}{l} \tag{21}$$

With the auxiliary functions k_{ij} the ratio of the real deflection shape (and later on the real twisting moment, the rotation and bending moment shapes) and a pure sine shape is approximated.

2. Twisting moment:

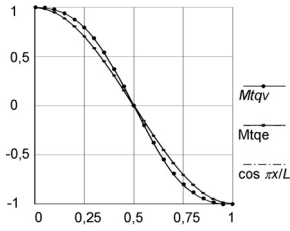


Figure 11b: M_{t2}

M_{t2} is calculated by integration of M'_{t2} - see (19).

$$M_{t2} = \int_{0.5l}^x (M_{y1}v'' + q_z e\varphi) d\xi \quad (22)$$

With the auxiliary functions k_{ij} this can be written as:

$$M_{t2} \cong \int_{0.5l}^x \left(-k_{1b} \bar{M}_{y1} \bar{v} \frac{\pi^2}{l^2} + k_{2a} \frac{\bar{M}_{y1}}{l^2} e\bar{\varphi} \right) \sin \frac{\pi \xi}{l} d\xi \text{ and results}$$

in:

$$M_{t2} \cong \left(k_{1c} \bar{M}_{y1} \bar{v} \frac{\pi}{l} - k_{2b} \frac{\bar{M}_{y1}}{\pi l} e\bar{\varphi} \right) \cos \frac{\pi x}{l} \quad (23)$$

3. Rotation of the cross-section: φ can be calculated by integration:

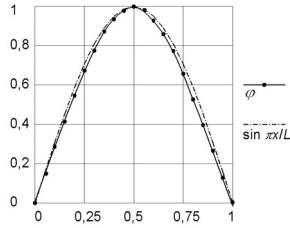


Figure 11c: φ

$$\varphi = \int_0^x \varphi' d\xi = \int_0^x \frac{M_{t2}}{GI_t} d\xi = \frac{k_{1d} \bar{M}_{y1} \bar{v} - k_{2c} \bar{M}_{y1} e\bar{\varphi}}{GI_t} \sin \frac{\pi x}{l} \quad (24)$$

with top value at: $x = 0.5l$:

$$\bar{\varphi} = \frac{k_{1d} \bar{M}_{y1} \bar{v} - k_{2c} \bar{M}_{y1} e\bar{\varphi}}{GI_t} = \frac{k_{1d} \bar{M}_{y1} \bar{v}}{GI_t + k_{2c} \bar{M}_{y1} e} \quad (25)$$

In Figure 11c it can be seen that the rotation shape accurately agrees with a pure sine shape.

4. 2nd-order moment:

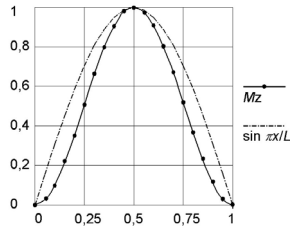


Figure 11d: M_{z2}

M_{z2} is obtained by: resolving of the moment M_{y1} , so: $M_{y1}\varphi$

axial force \times deflection, so: $F_c v$

$$M_{z2} = M_{y1} \varphi + F_c v = \left(\frac{(k_{1e} \bar{M}_{y1})^2}{GI_t + k_{2c} \bar{M}_{y1} e} + k_{1a} F_c \right) \bar{v} \sin \frac{\pi x}{l} \quad (26)$$

In Figure 11d the divergences are showed between the 2nd-order moment shape and a pure sine shape that has to be taken into account.

5. Curvature around the z-axis: The general relation between moment and curvature is:

$$v_2'' = -\frac{M_{z2}}{EI_z} = -\left(\frac{(k_{1e} \bar{M}_{y1})^2}{GI_t + k_{2c} \bar{M}_{y1} e} + k_{1a} F_c \right) \frac{\bar{v}}{EI_z} \sin \frac{\pi x}{l} \quad (27)$$

6. 2nd-order deflection:

v_2 is obtained from two times integration of the curvature:

$$v_2 = \int_0^x \int_{0.5l}^{\xi} v_2'' d\xi d\xi = \left(\frac{(k_{1e} \bar{M}_{y1})^2}{GI_t + k_{2c} \bar{M}_{y1} e} + k_{1a} F_c \right) \bar{v} \frac{l^2}{\pi^2 EI_z} \sin \frac{\pi x}{l}$$

7. The new deflection:

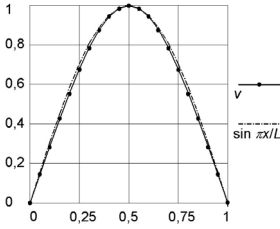


Figure 11e: v

Because in the analyzed case $k_{1a} \approx 1$ and the other auxiliary functions finally can be written as constant factors : k_1 respectively k_2 , the 2nd-order deflection becomes:

$$v_2 = \left(\frac{(k_1 \bar{M}_{y1})^2}{GI_t + k_2 \bar{M}_{y1} e} + F_c \right) \bar{v} \frac{l^2}{\pi^2 EI_z} \sin \frac{\pi x}{l} \quad (28)$$

Finally the total deflection is: $v = v_0 + v_2$

8. Check on similarity:

In spite of the in step 4 (Figure 11d) founded divergences between the 2nd-order moment shape and a pure sine shape it appears that (after two times integration) the final deflection shape closely agrees with the supposed deflection as started in step 1. Compare the Figures 11a and 11e.

9. The wanted quantity of the stability parameter n_z^* :

The ratio of \bar{v}_2 and \bar{v} is now most easily written in reciprocal form:

$$\frac{1}{n_z^*} = \frac{\bar{v}_2}{\bar{v}} = \left(\frac{(k_1 \bar{M}_{y1})^2}{GI_t + k_2 \bar{M}_{y1} e} + F_c \right) \frac{l^2}{\pi^2 EI_z} \quad (29)$$

From (14) it follows that the amplification factor runs to infinity for $n_z^* = 1$. The situation then has become critical. We will consider three cases for which $n_z^* = 1$ applies:

a. If the member is just loaded by an axial force F_c , a critical state is obtained, for which:

$$F_{c,cr} = \frac{\pi^2 EI_z}{l^2} \quad (30)$$

In this way the well-known Euler's buckling formula is derived from the displacements. It can be written:

$$F_{c,cr} = F_{Ez} \quad (31)$$

b. If the member is just loaded by a constant moment M_y the factor $k_1 = 1$ and a critical state is obtained, for which:

$$M_{y1,cr}^2 = \frac{\pi^2 EI_z GI_t}{l^2} = F_{Ez} GI_t \quad \text{or:}$$

$$M_{y1,cr} = \sqrt{F_{Ez} GI_t} \quad (32)$$

In the classical literature this is called the theoretical elastic flexural-torsional buckling moment, which often is written as:

$$M_{cr} = \frac{\pi}{l} \sqrt{EI_z GI_t} \quad (33)$$

c. At a combination of a constant bending moment and an axial force the stability parameter n_z^* can most easily be written with two (serially chained) components:

$$\frac{1}{n_z^*} = \frac{1}{n_{zM}^*} + \frac{1}{n_{zF}^*} \quad (34)$$

where:

$$n_{zM}^* = \frac{M_{cr}^2}{M_{y1}^2} \quad \text{and:} \quad n_{zF}^* = \frac{F_{Ez}}{F_c} \quad (35) \text{ and } (36)$$

If the moment will vary along the member and the load is applied eccentrically, the equations (34), (35) and (36) are still valid, however n_{zM}^* becomes:

$$n_{zM}^* = n_{zMcr}^* + n_{zM_e}^* \quad (37)$$

where:

$$n_{zMcr}^* = \left(\frac{M_{cr}}{k_1 \bar{M}_{y1}} \right)^2 \quad \text{and:} \quad n_{zM_e}^* = \frac{k_2 \bar{M}_{y1} e F_{Ez}}{(k_1 \bar{M}_{y1})^2} \quad \text{or:} \quad n_{zM_e}^* = \frac{e F_{Ez}}{k_2 \bar{M}_{y1}} \quad (38a), (38b), (38c)$$

where k_1 and k_2 are dimensionless constants.

In [14] several member types and load cases have been investigated, resulting into adequate values for these constants, listed in Table 5.

Table 5: Constants for the investigated member types and loads

Member type	Load	k_1	k_2	k'_2
two fork supports	constant moment M_{y1}	1	1	1
	homogeneously distributed load q_z	0,87	0,81	0,96
	concentrated mid-span load F_z	0,73	0,87	0,61
cantilever	constant moment M_{y1} ($e = 0$)	1	1	1
	homogeneously distributed load q_z	0.24	0.65	0.09
	concentrated end-of-span load F_z	0.41	0.57	0.29

It is concluded that the influences of the loads q_z and F_z (responsible for the moments \bar{M}_{y1}) and the eccentricity e act parallel, however the joint interaction of the compressive force F_c on the one hand and q_z , F_z and e on the other hand are chained serially. This is schematically visualized in Figure 12.

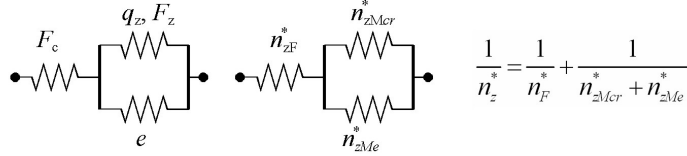


Figure 12: Scheme of serial and parallel interaction

Also combinations of different types of load, like moments in rigid supports and several concentrated loads, are investigated by iteration processes. In those cases it was observed that they can be accounted for by way of superposition using (38a) and (38b):

in the denominators of (38a) and (38b):

$$k_1 \bar{M}_{y1} = k_{1, \text{case1}} \bar{M}_{y1, \text{case1}} + k_{1, \text{case2}} \bar{M}_{y1, \text{case2}} + \dots \quad (39a)$$

in the numerator of (38b):

$$k_2 \bar{M}_{y1} e F_{Ez} = (k_{2, \text{case1}} \bar{M}_{y1, \text{case1}} e_{\text{case1}} + k_{2, \text{case2}} \bar{M}_{y1, \text{case2}} e_{\text{case2}} \dots) F_{Ez} \quad (39b)$$

Herein the eccentricity for the member deadweight is zero. The signs in all terms must be well chosen. Negative support moments have (in case of dominantly positive span moments) favorable effect on the stability, therefore they are subtracted. If so wished also values of the factors k may be calculated by interpolation in proportion to the loads. In this way n_z^* can be determined for most practical cases in a surveyable and rather simple way.

5 Check on strength and stiffness

For the purpose of applications in design practice checking criteria are mostly extracted from applying codes of practice. Because these codes are changed on a regular basis, we will refer to them as few as possible and, in stead, develop an autonomous calculation method for compressive-flexural-torsional buckling of members.

Having started from an initial deflection v_0 , the check is based on general principle for strength and stiffness, a simply to formulate, and applicable to structures in all kind of materials.

5.1 *Checking procedure*

We distinguish two limit states when judging stability, strength and stiffness of structures:

- ULS (ultimate limit state) for strength,
- SLS (serviceability limit state) for normative displacement.

The loads to account for in ULS (by way of load factors) are larger than in SLS, and the modulus of elasticity (dependent on the material) is sometimes smaller. As a consequence, the SLS-values of n^* are always larger than the ULS-values. In both limit states we can calculate the displacements with the same method.

The idea of the checking procedure is simple:

- ULS: it is investigated in which cross-section the normative design stress occurs, after which this stress is compared to the strength of the material (unity-check).
- SLS: it is investigated where the normative deflection occurs, after which this deflection is compared to the permissible one according to the applying requirements.

The necessary components are:

- external forces and moment: follow from equilibrium,
- geometric data: follow from beam theory,
- buckling stress: follows from Euler's formula,
- critical flexural-torsional moment: follows from lateral stiffness and torsion stiffness,
- initial eccentricity: follows from the nature of the material or from the code at stake,
- the quantity n^* : follows from the derived formulas in section 4,
- 2nd-order moments: follow from the derived formulas in section 5.

5.2 *Check on strength in the ULS*

In case of the here considered members, mainly bending stresses and (to a smaller degree) compressive stresses are relevant. Because they all act in axial direction of the member, they can simply be superimposed, as long as Hooke's law is applicable. See Figure 13.

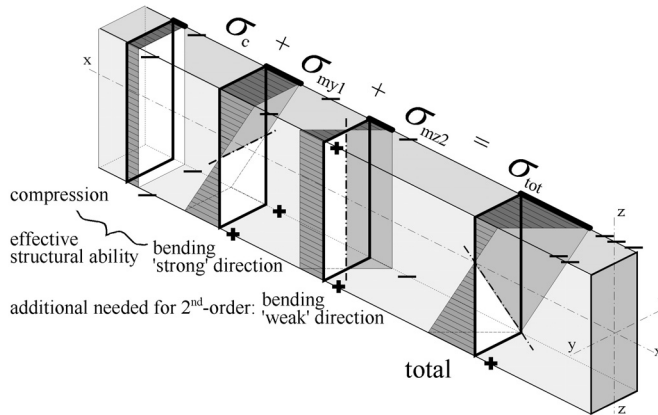


Figure 13: Superposition of stresses

In the normative position of the cross-section the ULS-strength can be checked with aid of:

$$\frac{F_c}{F_u} + \frac{\bar{M}_y}{M_{uy}} + \frac{\bar{M}_z}{M_{uz}} \leq 1 \quad (40)$$

The three quantities in the denominators are the respective ultimate design quantities.

As a rule, the moment \bar{M}_z is a 2nd-order moment. In general it holds:

$$\bar{M}_{z2} = -EI_z \bar{v}_2'' \quad (41)$$

Hence from: (27) and (28) \bar{M}_z can be short written as:

$$\bar{M}_{z2} = \frac{EI_z}{k_3} \frac{\pi^2}{l^2} \bar{v}_2 = \frac{F_{Ez} \bar{v}_2}{k_3} \quad (42)$$

where k_3 is a dimensionless factor, dependent on the shape of the M -diagram.

As commonly known, the shape and area of the moment diagram provides information on the size and the distribution of the deflections, and this holds true in the reversed direction as well. In case of a constant moment M_{y1} and/or a preponderant axial force (and so a sine shape of the v_2 diagram) the factor is: $k_3 = 1$. If the moment M_{y1} varies along the member, the factor has been studied for several load cases and support conditions in [14].

It appears that for members on two fork supports the value of k_3 is (practically) the same as the earlier calculated factor k_1 and that for cantilevers k_3 can be approximated with:

$$k_3 \cong k_1 + 0,8k_2 .$$

The calculation of \bar{M}_{z2} starts with the determination of n_z^* according to (34).

The relations between the initial deflection, the 2nd-order deflections and the total deflection result from (12) and (13):

$$\bar{v}_2 = \frac{\bar{v}}{n_z^*} = \frac{\bar{v}_0}{n_z^* - 1} \quad (43)$$

The value of \bar{v}_0 often can be extracted from the applying code of practice, and is - mostly - expressed in relation to the member length l (order of magnitude 1/1000 until 1/300).

So \bar{M}_{z2} can be written:

$$\bar{M}_{z2} = \frac{F_{Ez}}{k_3} \frac{\bar{v}_0}{n_z^* - 1} \quad (44)$$

This result is substituted in the checking formula (40).

This result is fine for rectangular cross-sections, but in members with an I-shaped cross-section one must account for an additional term. Because of the warping component M_{tw} in the torsion moment, flange bending moments occur. In members on two fork supports the maximum value occurs at mid-span, and to calculate the stresses we must use the section modulus $W_{flz} = 0,5 W_z$. Because the bending moments M_{y1} en M_{z2} are maximal at the same position as well, we best can consider $M_{z2,fl}$ to be a 'supplement' to M_{z2} .

In [14] it is derived for a member on two fork supports:

$$\frac{\bar{M}_{z2,fl}}{\bar{M}_{z2}} = \frac{F_{Ez} h}{4M_{y1}} \frac{n_z^*}{n_{zM}^*} \quad (45)$$

In absence of an axial compressive force this formula can be simplified to:

$$\frac{\bar{M}_{z2,fl}}{\bar{M}_{z2}} = \frac{F_{Ez} h}{4M_{y1}} \quad (46)$$

In total the moment in the middle of the member span can exist of two components:

1. A 2nd-order moment:

$$\bar{M}_{z2} = \frac{F_{Ez}}{k_3} \frac{\bar{v}_0}{n_z^* - 1} \quad \text{see (44)}$$

2. An additional 2nd-order component for I-sections,
due to flange bending:

$$\bar{M}_{z2,fl} = \frac{F_{Ez} h}{4M_{y1}} \frac{n_z^*}{n_{zM}^*} \bar{M}_{z2} \quad \text{see (45)}$$

(with section modulus $W_{flz} = 0,5 W_z$)

After all necessary components have been calculated, they are substituted in the checking formula (40).

Although it is a temptation to combine the foregoing formulas, we purposely abstain from that for easy reference.

5.3 Check on stiffness in the SLS

Stresses in the serviceability limit state are lower than in the ultimate limit state, 2nd-order effects are (much) smaller and sometimes the elasticity modulus is larger (in case of timber, for instance). Yet, the same formula's can be used.

The admissible deflection can be extracted from:

- applying codes of practice,
- additional requirements, due to the nature of the structure or special circumstances.

Mostly, these requirements regard the deflections in the direction of the load. It can be checked if the requirements are met with aid of n_y^* , through a procedure in three steps:

1. Calculation of the stability parameter n_y^* :
$$\frac{1}{n_y^*} = \frac{F_c}{F_{Ey}} \quad (47)$$

(which is influenced exclusively by an axial compressive force, and not by flexural-torsional effects)

1. Calculation of the normative deflection (in the middle of the member):
$$\bar{w} = (\bar{w}_0 + \bar{w}_1) \frac{n_y^*}{n_y^* - 1} + \text{creep effects} \quad (48)$$

3. Finally, checking by:
$$\bar{w} \leq w_{\text{allowable}} = \text{i.e. } 0.004 l \quad (49)$$

Dependent on the application, one could also distinguish between so called additional deflection (for variable load only) and total deflection (for both permanent and variable load).

A possible check on the deflections in the weak direction can be executed with the same calculation procedure in three steps:

1. Calculation of the quantity n_z^* :
$$\frac{1}{n_z^*} = \frac{1}{n_{zM}^*} + \frac{1}{n_{zF}^*} \quad \text{see (34)}$$

2. Calculation of the normative deflection:
$$\bar{v} = \bar{v}_0 \frac{n_z^*}{n_z^* - 1} + \text{creep effects} \quad (50)$$

3. Finally, checking by:
$$\bar{v} \leq v_{\text{allowable}} = \text{i.e. } 0.004 l \quad (51)$$

Also here again, possibly distinguishing between the additional and total deflection.

5.4 Sensitivity and accuracy

If structures become so slender that stresses due to 2nd-order effects start to be dominant, the state can become seriously dangerous. This is the case for values $n^* = 2$ à 3 or lower. As follows from (13) and all formula's derived thereof, the final deflections and stresses will

increase disproportionately at further increasing (variable) load and (as a consequence thereof) smaller values of n^* .

The determination of the stability parameters n_z^* and/or n_y^* provides good information about the 2nd-order effects and, therefore, is a valuable contribution to the design and construction of reliable structures.

6. Applications

The strength and stiffness of laterally supported members can be checked according to a conveniently-arranged procedure:

1. Collecting of data on the geometry of the considered member and the loads.
2. Choice of (reduction) factors, dependent on member type and load.
3. Determination of the needed components, dependent on member type and load.
4. Check if requirements for ULS and SLS are met.

6.1 Overview

In the overview below the procedures and formula's, derived in this article, are collected. For a more complete overview for other cases like members continuing over several supports and cantilever members, it is referred to [14].

a. Collection of data

items	notations	explanation
normative moment:	\bar{M}_{y1}	in the middle of the member.
initial deflection: in the weak direction	$\bar{v}_0 = k_{v0}l$	to be extracted from material properties and/or applying codes of practice. Order of magnitude:
also in the strong direction: (if necessary)	$\bar{w}_0 = \bar{v}_0$	$k_{v0} = 1/1000$ à $1/300$.
properties of the cross-section:	A b h I_y I_z I_{tor} W_y W_z etc.	to be extracted from structural mechanics formula's or tables.
material properties:	E G f_c f_m etc.	dependent on material.
eccentricity of the load:	e	positive in direction of load.

b. Choice of constants, depending on member type and load:

member type	loaded by		k_1	k_2	k'_2	k_3
member on two	constant moment	($e = 0$)	1	1	1	1
fork supports:	homogeneously distributed load	q_z	0.88	0.81	0.96	0.88
	concentrated load at mid-span	F_z	0.73	0.87	0.61	0.73
cantilever:	constant moment	M_{y1} ($e = 0$)	1	1	1	1
	homogeneously distributed load	q_z	0.24	0.65	0.09	0.79
	concentrated end-of-span load	F_z	0.41	0.57	0.29	0.85

c. Involved quantities and formulas:

Euler buckling load:	$F_{Ez} = \frac{\pi^2 EI_z}{l^2}$	ditto in strong direction (if wanted)	$F_{Ey} = \frac{\pi^2 EI_y}{l^2}$
torsion stiffness::	$GI_t = GI_{tor} (1 + C_{tw})$	for rectangular cross-sections: for I-sections:	$C_{tw} = 0$ $C_{tw} = \frac{\pi^2 EI_z h^2}{4GI_{tor} l^2}$
critical flexural-torsional moment:	$M_{cr} = \sqrt{F_{Ez} GI_t}$		
stability parameter:	$\frac{1}{n_z^*} = \frac{1}{n_{zM}^*} + \frac{1}{n_{zF}^*}$	components related to moment:	$n_{zM}^* = n_{zMcr}^* + n_{zMe}^*$ $n_{zMcr}^* = \left(\frac{M_{cr}}{k_1 \bar{M}_{y1}} \right)^2$ $n_{zMe}^* = \frac{k_2 e F_{Ez}}{k_1^2 \bar{M}_{y1}} = \frac{e F_{Ez}}{k_2' \bar{M}_{y1}}$
combination of different loading types (substitute with correct sign)		$k_1 \bar{M}_{y1} = \sum k_{1,i} \bar{M}_{y1,i}$ $k_2 \bar{M}_{y2} e = \sum k_{2,i} \bar{M}_{y2,i} e$	i = case 1, case 2, etc. respectively
2 nd -order moment:	$\bar{M}_{z;tot} = \bar{M}_{z2} + 2\bar{M}_{z2;fl}$	bending moment: flange bending moment: (for I-sections only) section modulus $W_{flz} = 0,5W_z$)	$\bar{M}_{z2} = \frac{F_{Ez} \bar{v}_0}{k_3 (n_z^* - 1)}$ $\bar{M}_{z2;fl} = \frac{F_{Ez} h}{4\bar{M}_{y1}} \frac{n_z^*}{n_{zM}^*} \bar{M}_{z2}$
stability parameter (if wanted) in 'strong' direction:		$n_y^* = n_{yF}^* = \frac{F_{Ey}}{F_c}$	

d. Checking

ULS	strength: calculation for ULS-load		$\frac{F_c}{F_u} + \frac{\bar{M}_{y1}}{M_{ly}} + \frac{\bar{M}_{z202}}{M_{lz}} \leq 1$
SLS	deflection: calculation for SLS-load	in the 'strong' direction:	$\bar{w} = (\bar{w}_0 + \bar{w}_1) \frac{n_y^*}{n_y^* - 1} \quad \text{where: } \frac{1}{n_y^*} = \frac{F_c}{F_{Ey}}$ $\bar{w} \leq \bar{w}_{\text{allowable}} = \text{i.e. } 0.004 l$
	possibly distinguishing between additional and total deflection	if wanted in the 'weak' direction:	$\bar{v} = \bar{v}_0 \frac{n_z^*}{n_z^* - 1} \quad \text{where: } \frac{1}{n_z^*} = \frac{1}{n_{zM}^*} + \frac{1}{n_{zF}^*}$ $\bar{v} \leq \bar{v}_{\text{allowable}} = \text{i.e. } 0.004 l$

6.2 Calculation example

To illustrate the procedure a calculation example will be shown. We consider a steel member on two fork supports under a homogeneously distributed load and axial compressive force, see Figure 14.

The calculation exists of two parts:

- one that has to be executed regardless of the chosen method, whatsoever, and
- one that is specifically focused to the method developed in this article.

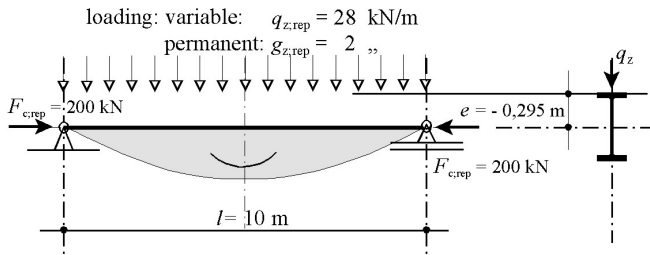


Figure 14 I-beam under representative uniform loading

6.2.1 a. Data

member length:	$l = 10$	[m]	Section data, extracted from
section HE600A:	$h = 0.590$ and $b = 0.300$	„	tables for steel sections:
initial deflection:	$\bar{v}_0 = 10/500 = 0.020$	„	

loads:	in the SLS:	in the ULS:	$A = 22646 \times 10^{-6}$	[m ²]
deadweight:	$q_w = 2$	2.4 [kN/m]	$I_y = 1412 \times 10^{-6}$	[m ⁴]
variable, distributed:	$q_z = 28$	42 [kN/m]	$I_z = 113 \times 10^{-6}$	[m ⁴]
compressive force:	$F_c = 200$	300 [kN]	$I_{tor} = 3.5 \times 10^{-6}$	[m ⁴]
eccentricity of load	$e = -0.590/2 = -0.295$	[m]	$I_w = 9 \times 10^{-6}$	[m ⁶]
	(here for variable load only)		$W_y = 4787 \times 10^{-6}$	[m ³]
material data:	$E = 210 \times 10^6$	[kN/m ²]	$W_z = 751 \times 10^{-6}$	[m ³]
	$G = 0.4E = 84 \times 10^6$	„		
checking criteria:	ULS	total stress:	$f_{tot} \leq f_y = 0.235 \times 10^6$	[kN/m ²]
	SLS	total deflection: additional deflection:	$\left. \begin{array}{l} \bar{w} - \bar{w}_0 = \bar{w}_1 + \bar{w}_2 \\ \bar{v} - \bar{v}_0 = \bar{v}_2 \end{array} \right\} \leq 0.004l =$	
			$= 0.0040 \times 10 = 0.040$	[m]

b. Elaboration

design values	SLS	$\bar{M}_{y1,rep} = \frac{1}{8}(2.0+28)10^2 = 25 + 350 = 375$	[kNm]
moments and			
eccentricities :		$e = -0.295 \times \frac{28}{2+30} = -0.275$	[m]
	ULS	$\bar{M}_{y1,rep} = \frac{1}{8}(2.4+42)10^2 = 30 + 525 = 555$	[kNm]
		$e = -0.295 \times \frac{42}{2.4+42} = -0.279$	[m]
ultimate normal	$F_u = 0.235 \times 22646 = 5322$		[kN]
force	$M_{yu} = 0.235 \times 4787 = 1125$		[kNm]
and moments:	$M_{zu} = 0.235 \times 751 = 176$		[kNm]
Euler buckling	$F_{Ez} = \frac{\pi^2 \times 210 \cdot 10^6 \times 113 \cdot 10^{-6}}{10^2} = 2342$		[kN]
load:			
torsion stiffness:	$GI_{tor} = 84 \cdot 10^6 \times 3.5 \cdot 10^{-6} = 294$		
warping stiffness:	$EI_w = 210 \times 9 = 1890$		[kNm ²]
	$C_{nw} = \frac{\pi^2 \times 1890}{10^2 \times 294} = 0.63$		[kNm ⁴]
effective torsion			[--]
stiffness:	$GI_t = 294(1+0.63) = 480$		[kNm ²]
critical flexural-	$M_{cr} = \sqrt{2342 \times 480} = 1060$		[kNm]
torsional moment:			[kNm]

So far the calculation does not differ from usual approaches in codes.

Now it is followed by a part for the calculation and checking of the strength and stiffness conform the method developed in this article.

6.2.2 a. ULS - strength

factors:	$k_1 = 0.88$ $k_2 = 0.81$ $k'_2 = 0.96$ (from Table 5)
stability parameter n_z^*	$\left[\begin{aligned} n_{zM}^* &= \left(\frac{1060}{0.88 \times 555} \right)^2 + \frac{-0.275 \times 2342}{0.96 \times 555} = 3.5 \\ n_{zF}^* &= \frac{2342}{30} = 7.8 \end{aligned} \right.$ <p>alternative:</p> $\left[\begin{aligned} \frac{1}{n_{zM}^*} &= \frac{(0.88 \times 555)^2}{1060^2 + (0 - 0.81 \times 525 \times 0.295) \times 2342} = \frac{1}{3.5} \\ \frac{1}{n_{zF}^*} &= \frac{300}{2342} = \frac{1}{7.8} \\ \frac{1}{n_z^*} &= \frac{1}{3.5} + \frac{1}{7.8} = \frac{1}{2.4} \end{aligned} \right.$
comment, alarming function:	This size of the stability parameter n_z^* definitely requires reconsidering the design critically, because the 2 nd -order amplification factor of $\frac{2.4}{2.4-1} = 1.71$ is rather large.
2 nd -order bending moment:	$\bar{M}_{z2} = \frac{2342 \times 0,020}{0.88(2.4-1)} = 38$ [kNm]
flange bending moment:	$\bar{M}_{z2;fl} = \frac{2342 \times 0,590}{4 \times 555} \times \frac{2.4}{3.5} \times 38 = 16$ [kNm]
Seldom attention is paid to the flange bending moment $M_{z2;fl}$, that roughly is related to the 2 nd -order moment M_{z2} by the warping factor C_{tw} . This moment must be carried per flange, so half the section modulus in the weak direction is used.	
check:	$\frac{300}{5322} + \frac{555}{1125} + \frac{38}{176} + \frac{16}{0.5 \times 176} = 0.06 + 0.50 + 0.21 + 0.18 = 0.95 < 1$
comment:	the extra stress due to the 2 nd -order contribution is: $\frac{0,21+0,18}{0,06+0,50} \Rightarrow 70\%$ which agrees well with the amplification factor 1.67, found before.
Indeed, the checking result $0.95 < 1$ is satisfactory, but the size of n_z^* yet is a reason to be wakeful. The safety may seem 5%, however this is very relative, for an increase in load would yield a disproportionate raise of the checking value 0.95. An increase of the load of 5% makes the checking value 1.04, which is an increase of 9%, almost the double.	

For reasons of illustration it is investigated in which way the checking value develops at increasing load. The result is shown in Figure 15.

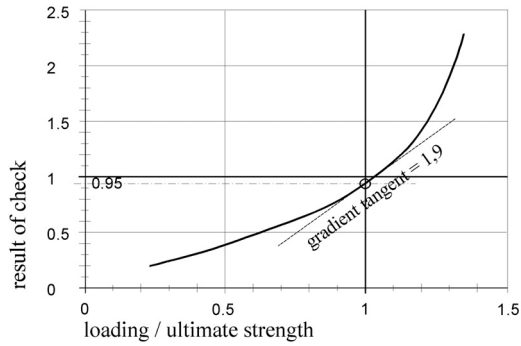


Figure 15: Increasing check result for increasing loading

The axes indicate:

- horizontal: ratio of the load and the design load
- vertical: the checking value.

The circled point marks the result of the preceding calculation with checking value 0.95.

From the graph the following conclusions are drawn:

- A safe result is found for small loads.
- The checking value grows progressively for increasing loads.
- Therefore, thinking in terms of a linear relation is dangerous.

b. SLS - 1. stiffness in the strong direction

The deflections can be calculated according section 5.3

First determination of Euler buckling force:	$F_{Ey} = \frac{\pi^2 \times 210 \cdot 10^6 \times 1412 \cdot 10^{-6}}{10^2} = 29265$	[kN]
and deflection 1 st -order:	$\bar{w}_1 = \frac{5 \times 375 \times 10^2}{48 \times 210 \cdot 10^6 \times 1412 \cdot 10^{-6}} = 0.013$	[m]
stability parameter n_y^* :	$n_y^* = \frac{29265}{200} = 146$	
normative deflection:	$\bar{w} = (0.020 + 0.013) \frac{146}{146 - 1} = 0.033$	[m]
check:	$\bar{w} - \bar{w}_0 = 0.033 - 0.020 = 0.013 \leq 0.040$	[m]

2. stiffness in the weak direction

This calculation will not be often necessary, but can be executed (if wanted) with:

stability parameter n_z^* :	$\left[\begin{array}{l} n_{zM}^* = \left(\frac{1060}{0.88 \times 375} \right)^2 + \frac{-0.279 \times 2342}{0.96 \times 375} = 8.5 \\ n_{zF}^* = \frac{2342}{200} = 11.7 \end{array} \right.$	
	alternative:	
	$\left[\begin{array}{l} \frac{1}{n_{zM}^*} = \frac{(0.88 \times 375)^2}{1060^2 + (0 - 0.81 \times 350 \times 0.295) \times 2342} = \frac{1}{8.5} \\ \frac{1}{n_{zF}^*} = \frac{200}{2342} = \frac{1}{11.7} \end{array} \right.$	
	$\frac{1}{n_z^*} = \frac{1}{8.5} + \frac{1}{11.7} = \frac{1}{4.9}$	
normative deflection:	$\bar{v} = 0.020 \times \frac{4.9}{4.9 - 1} = 0.025$	[m]
check:	$\bar{v} - \bar{v}_0 = 0.025 - 0.020 = 0.005 \leq 0.040$	[m]

7 Conclusions and recommendations

7.1 Conclusions

1. The developed stability parameter n^* can have a very important 'alarming function' in the assessment of the stability behavior of members. Therefore, it is strongly recommended to pay careful attention to the size of n_z^* , and take care that it does not become smaller than 2 à 3.
2. It's true, this role of n^* is not completely unknown, but was not given a place in regulations on flexural-torsional buckling in the consulted building codes and literature. At increasing load approaching the critical value, sudden loss of stability (and failure of the structure) may occur. Clearly, the 'unsuspecting' application of checking rules which do not show this is dangerous.

3. A method for compressive-flexural-torsional buckling has been derived, applicable to all existing building materials in structural engineering for which plasticity considerations do not influence the beam-column buckling load to a substantial extent.
4. Essentially the calculations can be done in a short time using a pocket calculator, without the use of other utilities.
5. It has been deliberately chosen not to elaborate the derived formulas too far, in order to preserve a clear view on the cohesion and procedure.

7.2 *Recommendations*

1. It is desirable and possible to apply to all building materials the same calculation system for the checking regulations regarding stability, stiffness and strength of members, which are loaded in bending and compression.
2. Apart of the cases mentioned in [14], larger applications should be investigated which adaptations are necessary for:
 - other than straight, prismatic members (i.e. curved and/or tapered members), members with other cross-section shapes, sloped frames and also cracked reinforced concrete cross-sections.
 - materials for which the theory of elasticity does not apply, for instance plastic behavior.

References

- [1] Timoshenko, S. *Theory of elastic stability*, (1st edition) New York, 1936.
- [2] Timoshenko, S. and Geere, J.M., *Theory of elastic stability*, New York, 1961.
- [3] Bleich, F., *Buckling Strength of Metal Structures*, McGraw-Hill, 1952.
- [4] Chen, W.F. and Atsuta, T., *Theory of beam-columns*, vol. 2. Space behavior and design, New York, 1977.
- [5] Bazant, Z. P. and Cedolin, L., *Stability of Structures: Elastic, Inelastic Fracture and Damage Theories*, Oxford University Press, New York, 1991
- [6] Trahair, N.S. *Flexural-torsional buckling of structures*, London, 1993.

- [7] Brüninghoff, H., *Spannungen und Stabilität bei quergestützten Brettschichtträgern*, Karlsruhe, 1972.
- [8] Blass, H.J., *Tragfähigkeit von Druckstäben aus Brettschichtholz unter Berücksichtigung streuender Einflussgrößen*, Karlsruhe, 1987.
- [9] Pauli, W., *Versuche zur Kippstabilität an praxisgerechten Fertigteilträgern aus Stahlbeton und Spannbeton*, Darmstadt, 1990.
- [10] Lohse, G., *Kippen*, Düsseldorf, 1997.
- [11] Eggen, T.E., *Buckling and geometrical nonlinear beam-type analyses of timber structures*, Trondheim, 2000.
- [12] Van der Put, T.C.A.M., *Stability of beams (background of Dutch code TGB) Chapter KH 10 in PAO Continuing Education Course "Structures in timber"*, Delft 1992. (Title of the chapter is in Dutch: Stabiteit van liggers (achtergrond TGB) in Cursus 'Constructies in hout'. Text of the chapter is in English).
- [13] Erp, G.M. van, *Advanced buckling analyses of beams with arbitrary cross-sections*, Eindhoven, 1989.
- [14] Raven, W.J., *New vision on flexural-torsional buckling. Stability and strength of structural members* (in Dutch: Nieuwe blik op kip en knik, Stabiteit en sterkte van staven), doctoral thesis, Delft 2006. To download from TU-Delft library:
<http://repository.tudelft.nl/file/204111/173135>
- [15] TGB 1990, *NEN 6700*, and successive supplements, Dutch building code.

Appendix

Notations

In this article the following symbols are used:

Geometry of member

l	length	[m]
A	area of cross-section	[m ²]
A_{fl}	area of flange	[m ²]
b	width of cross-section	[m]
h	depth of cross-section	[m]
e	eccentricity of load in z-direction	[m]
x, y, z	variables along the coordinate axes	[m]
ξ, ζ	auxiliary variables (along the x-axis)	[m]

Static properties

I_y, I_z	second moment of cross-section for bending corresponding with M_y and M_z	[m ⁴]
I_{tor}	second moment for torsion at no restrained warping	[m ⁴]

I_t	idem, restrained warping included	[m ⁴]
I_w	bimoment of cross-section	[m ⁶]
W	section modulus for bending	[m ³]
<i>Material properties</i>		
E	modulus of elasticity	[N/m ²]
G	shear modulus	[N/m ²]
f_c	compressive strength	[N/m ²]
f_m	strength in bending	[N/m ²]
<i>Stiffness and strength</i>		
C_{tw}	dimensionless quantity for the influence of the warping stiffness	[--]
F_E	Euler buckling load	[N]
F_u	ultimate compressive strength F_c	[N]
M_{cr}	critical moment M at flexural-torsional buckling	[Nm]
M_u	ultimate moment M at bending	[Nm]
n	stability parameter (applied in classical theory of Eulerian buckling)	[--]
n^*	stability parameter (newly introduced in this article)	[--]
<i>Loads, moments and shear forces</i>		
q_z	load per unit length (in z-direction)	[N/m]
F	concentrated load	[N]
F_c	axial compressive force in x -direction	[N]
M_x	twisting moment in cross-section around the x -axis	[Nm]
M_y	bending moment in cross-section around the y -axis	[Nm]
M_z	bending moment in cross-section around the z -axis	[Nm]
M_t	twisting moment in cross-section around member axis	[Nm]
V	shear force in cross-section	[N]
<i>Stresses</i>		
σ_c	compressive stress	[N/m ²]
σ_m	bending stress	[N/m ²]
τ	shear stress	[N/m ²]
<i>Displacements</i>		
w	displacement in z -direction	[m]
v	displacement in y -direction	[m]
v_0	initial displacement in y -direction	[m]
v_1	first-order displacement in y -direction	[m]
v_2	second-order displacement in y -direction	[m]
φ	rotation of a member cross-section around the x -axis	[rad]
φ'	torsion = rotation per unit length	[rad/m]
<i>Auxiliary quantities</i>		
k	constant, factor, coefficient	[--]
k_i	reduction factor ($i = 1, 2, 3, \dots$)	[--]
\bar{f}	in general: a dash on top of a symbol indicates the maximum value of the considered function in case of moments, stresses and displacements.	